

Chapter 2

Basic thermodynamic and acoustic concepts

This chapter presents the underlying thermodynamic and acoustic principles, and discusses the interplay of these effects in thermoacoustics. The chapter starts with a review of the thermodynamic efficiency of a heat engine and the coefficient of performance of a refrigerator and heat pump. Then, a description of the thermodynamics of the gas oscillating in the channels of a stack will be introduced. Simple expressions for the heat flow and acoustic power used in the stack will be derived. After that, the acoustics of thermoacoustic devices will be illustrated, and the important concepts for the operation will be explained. Finally, some basic measurements with a simple thermoacoustic refrigerator will be used to clarify the discussed effects.

2.1 Thermodynamic performance

In this section the thermal efficiency for prime movers and the coefficient of performance for refrigerators and heat pumps are introduced, using the first and second law of thermodynamics.

From the thermodynamic point of view, prime movers are devices that, per cycle, use heat Q_H from a source at a high temperature T_H and reject waste heat to a source at a lower temperature T_C , to generate work W . On the other hand, refrigerators and heat pumps are devices that use work W to remove heat Q_C at a temperature T_C and reject Q_H at a higher temperature T_H . These devices are illustrated in Fig.(2.1).

The energy flows into and out of thermodynamic systems are controlled by the first and second law of thermodynamics. The first law of thermodynamics is a statement of the energy conservation: the rate of increase or decrease of the internal energy \dot{U} of a thermodynamic system of volume V equals the algebraic sum of the heat flows, and

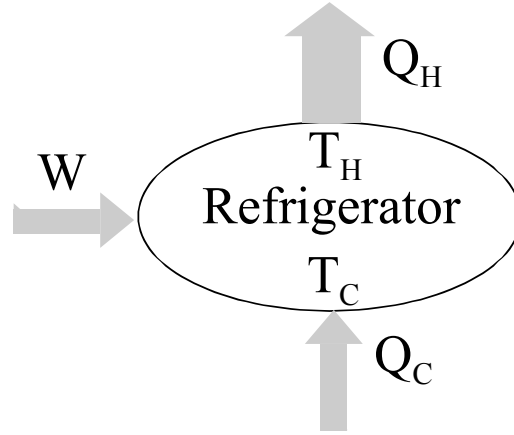


Figure 2.1: Representation of a refrigerator while exchanging per cycle heat and work with the surroundings. The directions of heat and work exchanged between the refrigerator and its environment are shown by the shaded arrows. In a prime mover the directions of the arrows are reversed.

enthalpy flows into the system, minus the work done by the system on the surroundings [1]

$$\dot{U} = \Sigma \dot{Q} + \Sigma \dot{n} H_m - p \dot{V} + P \quad (2.1)$$

where \dot{n} is the molar flow rate of matter flowing into the system, H_m is the molar enthalpy, and P represents other forms of work done on the system. The summations are over the various sources of heat and mass in contact with the system; transfers into the system are positive and those out of the system are negative.

The second law of thermodynamics limits the interchange of heat and work in thermodynamic systems. This law states that the rate of change of entropy of a thermodynamic system is equal to the algebraic sum of the entropy change due to the heat flows, due to the mass flows, and due to the irreversible entropy production in the system [1]

$$\dot{S} = \Sigma \frac{\dot{Q}}{T} + \Sigma \dot{n} S_m + \dot{S}_i, \quad (2.2)$$

where the summation is over the various sources with the same sign convention as stated above. The heat flow, \dot{Q} , into or out of the system, takes place at the temperature T . In addition the second law of thermodynamics requires that

$$\dot{S}_i \geq 0. \quad (2.3)$$

In the following the first and second law of thermodynamics, Eqs.(2.1)-(2.3), will be used to define the performance for refrigerators, heat pumps and prime movers.

2.1.1 Refrigerators and heat pumps

The duty of a refrigerator or heat pump, is to remove a heat quantity Q_C at a low temperature T_C and to supply a heat quantity Q_H to the surroundings at a high temperature T_H . To accomplish these processes a net work input, W , is required. This process is illustrated in Fig.(2.1). Refrigerators and heat pumps have different goals. The goal of a refrigerator is to maintain the temperature of a given space below that of the surroundings. While the goal of a heat pump is to maintain the temperature of a given space above that of the surroundings. Since refrigeration and heat pump systems have different goals, their performance parameters, called coefficient of performance (COP) are defined differently.

By considering the refrigerator illustrated in Fig.(2.1) and using the fact that there is no mass flow into or out of the system, the first and second law, Eqs.(2.1) and (2.2), take the simple form

$$\dot{U} = \dot{Q}_C - \dot{Q}_H + \dot{W}, \quad (2.4)$$

and

$$\dot{S} = \frac{\dot{Q}_C}{T_C} - \frac{\dot{Q}_H}{T_H} + \dot{S}_i, \quad (2.5)$$

where U and S are the internal energy and entropy of the system, respectively; \dot{S}_i is the irreversible entropy production in the system. The integration over one cycle of Eqs.(2.4) and (2.5), and the use of the fact that U and S are functions of state which do not change over one cycle, yields

$$Q_H = Q_C + W \quad (2.6)$$

and

$$\frac{Q_H}{T_H} = \frac{Q_C}{T_C} + S_i. \quad (2.7)$$

Refrigerator

In the case of a refrigerator we are interested in the heat removed Q_C at T_C , and the net work used to accomplish this effect, W . The COP_{ref} is given by the ratio of these quantities, thus

$$COP_{\text{ref}} = \frac{Q_C}{W}. \quad (2.8)$$

Substituting Eq.(2.6) into Eq.(2.8) yields

$$COP_{\text{ref}} = \frac{Q_C}{Q_H - Q_C}. \quad (2.9)$$

Since $S_i \geq 0$, Eq.(2.7) gives

$$\frac{Q_C}{T_C} \leq \frac{Q_H}{T_H}. \quad (2.10)$$

Combining Eq.(2.9) with Eq.(2.10) gives

$$COP_{\text{ref}} \leq \frac{T_C}{T_H - T_C}. \quad (2.11)$$

The quantity

$$COPC = \frac{T_C}{T_H - T_C} \quad (2.12)$$

is called the Carnot coefficient of performance which is the maximal performance for all refrigerators. This COP can be made larger than one if $T_C > T_H/2$. The coefficient of performance relative to Carnot's coefficient of performance is defined as

$$COPR = \frac{COP}{COPC}. \quad (2.13)$$

Heat pump

The performance of heat pumps is defined as the ratio of the desired heat, Q_H , to the net work needed W . For a heat pump we are interested in the heat Q_H supplied to a given space. Thus the coefficient of performance, COP_{hp} , is

$$COP_{\text{hp}} = \frac{Q_H}{W}. \quad (2.14)$$

In combination with Eq.(2.6), this gives

$$COP_{\text{hp}} = \frac{Q_H}{Q_H - Q_C}. \quad (2.15)$$

This expression shows that the value of the COP_{hp} is always larger than unity. Combining Eq.(2.15) and Eq.(2.10) leads to the expression

$$COP_{\text{hp}} \leq \frac{T_H}{T_H - T_C}. \quad (2.16)$$

The temperature expression on the right is called the Carnot COP_{hp} which is the maximal performance for all heat pumps.

The coefficients of performance COP_{ref} and COP_{hp} are defined as ratios of the desired heat transfer output to work input needed to accomplish that transfer. Based on the definitions given above, it is desirable thermodynamically that these coefficients have values that are as large as possible. As can be seen from Eqs.(2.11), (2.16), the second law of thermodynamics imposes limits on the performance, because of irreversibilities in the system.

2.1.2 Efficiency of the prime mover

Since the prime mover uses heat Q_H to produce work W the directions of heat and work flows in Fig.(2.1) are reversed. The performance η of a prime mover is defined as the ratio of the produced work (output) and the heat used to produce that work (input), thus

$$\eta = \frac{W}{Q_H}. \quad (2.17)$$

By use of Eq.(2.6), we have

$$\eta = \frac{Q_H - Q_C}{Q_H}. \quad (2.18)$$

This expression shows that the efficiency of a prime mover is less than one. Since Q_H is entering the prime mover and Q_C is flowing out of it, Eq.(2.10) becomes

$$\frac{Q_C}{T_C} \geq \frac{Q_H}{T_H}. \quad (2.19)$$

In a similar way as described above, we can derive the well-known relation

$$\eta \leq 1 - \frac{T_C}{T_H}. \quad (2.20)$$

The temperature expression on the right is called the Carnot efficiency, which is the maximal performance for all prime movers.

2.2 Thermodynamic approach to thermoacoustics

A simplified picture of the thermoacoustic effect will be given, using only thermodynamics and acoustics to explain how a temperature gradient, and hence cooling, develops across a stack. The discussion in this section is concerned with the derivation of approximative expressions for the critical temperature gradient and the heat and work flows in thermoacoustic devices. The papers of Wheatley et al.[2] and Swift [3] form the basis for the discussion in this section. Most of the matter and illustrations discussed in chapter 1, will be repeated here for ease of discussion and derivation of thermoacoustic quantities.

As discussed in the preceding chapter, thermoacoustic devices consist mainly of an acoustic resonator filled with a gas. In the resonator, a stack consisting of a number of parallel plates, and two heat exchangers, are appropriately installed (Fig.(2.2a)). The stack is the element in which the heat-pumping process takes place. The heat exchangers are necessary to exchange heat with the surroundings, at the cold and hot sides of the stack, as shown in Fig.(2.2a). A loudspeaker sustains an acoustic standing

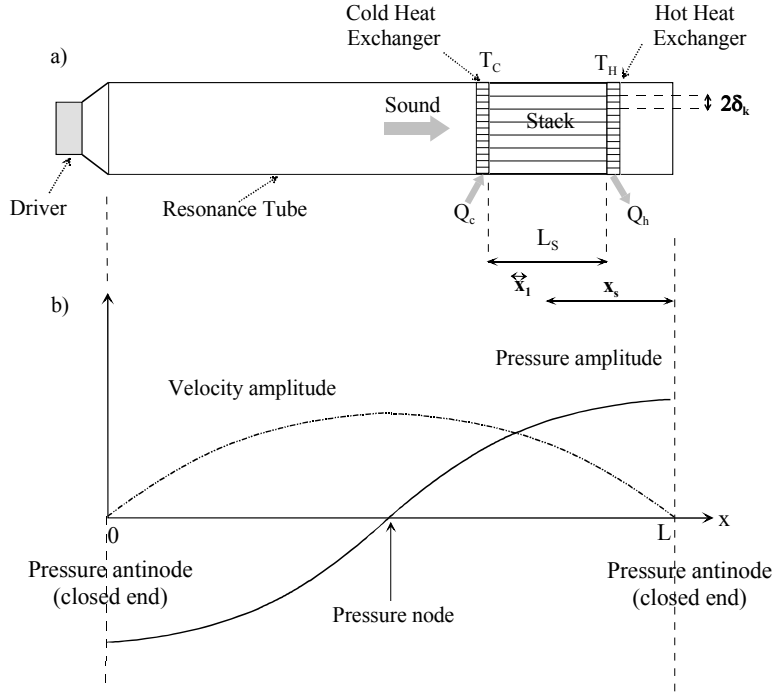


Figure 2.2: *Model of a thermoacoustic refrigerator. a) An acoustically resonant tube containing a gas, a stack of parallel plates and two heat exchangers. An acoustic driver is attached to one end of the tube and the other end is closed. Some length scales are also shown: the gas excursion in the stack x_1 , the length of the stack L_s , the position of the center of the stack from the closed end x_s and the spacing in the stack $2\delta_k$. b) Illustration of the standing wave pressure and velocity in the resonator.*

wave in the acoustic resonator. As an approximation, we neglect the viscosity of the gas and the longitudinal thermal conductivity. In response to the acoustic wave, the gas oscillates in the stack channels and is compressed and expanded.

We begin by discussing the thermodynamics of a small parcel of gas oscillating along a stack plate, being compressed and expanded by the sound wave. An average longitudinal temperature gradient ∇T_m along the stack is supposed to exist. Additionally, we suppose that the pressure antinode is to the right of the plate and a node to the left (Fig.(2.2b)). For simplicity, the following treatment will assume an inviscid ideal gas of vanishing Prandtl number. A more complete theory that includes viscosity is postponed until Chapter 3.

The four steps of the thermoacoustic cycle are illustrated separately in Fig.(2.3). We suppose that, in the start of the cycle, the temperature, pressure, and volume of the parcel are $T_m - x_1 \nabla T_m$, $p_m - p_1$, and V . In step 1, the parcel of gas moves a distance $2x_1$, is compressed and increases in temperature by an amount $2T_1$. The adiabatic

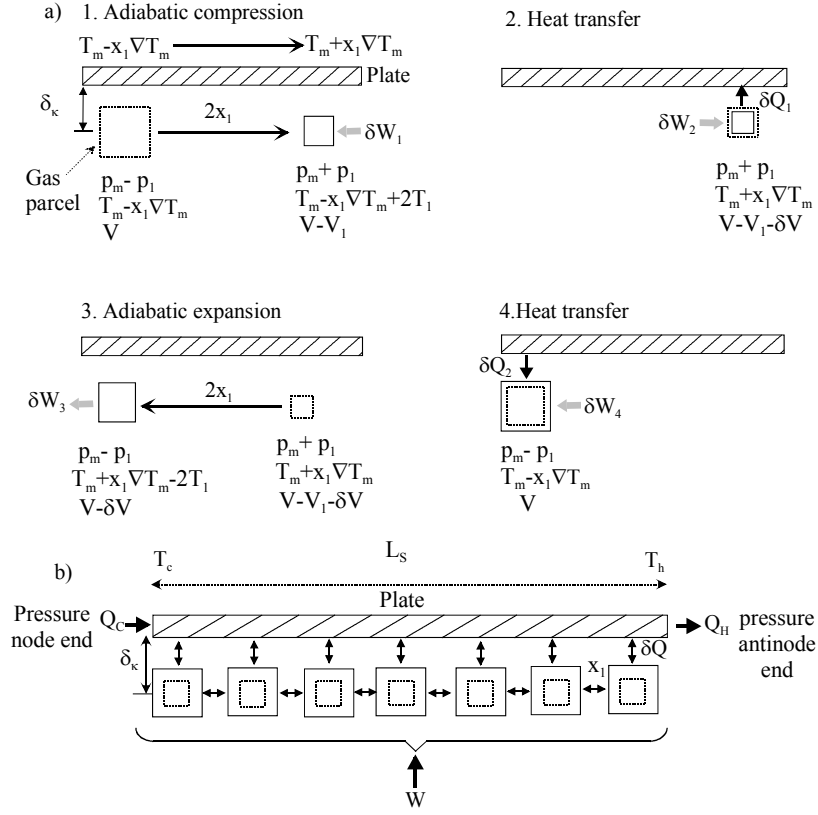


Figure 2.3: a) Typical gas parcel in a thermoacoustic refrigerator passing through a four-step cycle with two adiabats (step 1 and 3) and two constant-pressure heat transfer steps (steps 2 and 4). b) An amount of heat is shuttled along the stack plate from one parcel of gas to the next, as a result heat Q is transported from the left end of the plate to the right end, using work W . The heat increases in the stack from Q_c to Q_h (Eq.(2.6)).

pressure change p_1 and temperature change T_1 are related by the thermodynamic relationship

$$Tds = c_p dT + \frac{T}{\rho^2} \left(\frac{\partial \rho}{\partial T} \right)_p dp = 0, \quad (2.21)$$

where s is the specific entropy, ρ is the density, c_p is the isobaric specific heat per unit mass, T is the absolute temperature, and p is the pressure. This expression can be rewritten as

$$T_1 = \left(\frac{\beta T}{\rho c_p} \right)_m p_1 \quad (2.22)$$

where

$$\beta = -\frac{1}{\rho} \left(\frac{\partial \rho}{\partial T} \right)_p. \quad (2.23)$$

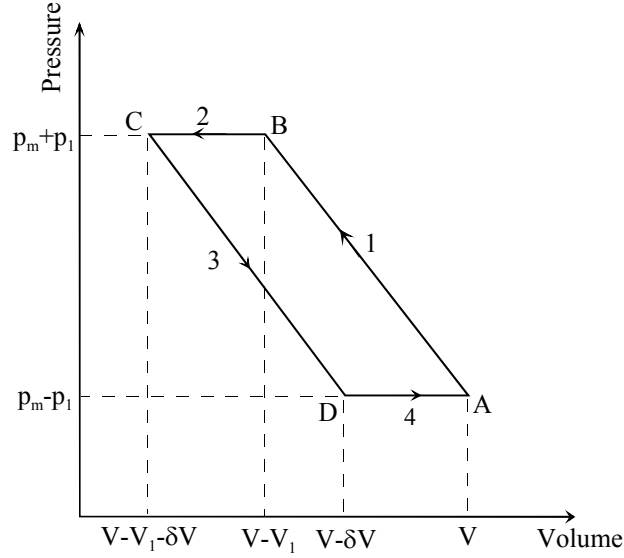


Figure 2.4: Schematic pV -diagram of the thermoacoustic cycle of Fig.(2.3). The four steps of the thermoacoustic cycle are illustrated: adiabatic compression (1), isobaric heat transfer (2), adiabatic expansion (3) and isobaric heat transfer (4). The area $ABCD$ is the work used in the cycle which is also equal to the sum of the works used in the different steps.

The subscript m indicates that we are concerned with the mean value of the quantities between brackets. The parameter β is the isobaric volumetric expansion coefficient. Considering an ideal gas ($\beta T_m = 1$) and using the ideal gas law, the expression (2.22) becomes

$$\frac{T_1}{T_m} = \frac{\gamma - 1}{\gamma} \frac{p_1}{p_m}, \quad (2.24)$$

where γ is the ratio of isobaric to isochoric specific heats.

After the displacement and compression in step 1, the temperature, pressure and volume becomes $T_m - x_1 \nabla T_m + 2T_1$, $p_m + p_1$, and $V - V_1$. At this time, the temperature difference between the plate and the parcel of gas is

$$\delta T = 2T_1 - 2x_1 \nabla T_m, \quad (2.25)$$

where $2x_1 \nabla T_m$ is the temperature change along the plate. In step 2, for positive δT , heat δQ flows from the parcel of gas to the plate at constant pressure. The heat that flows out of the parcel is given by

$$\delta Q \approx mc_p \delta T \quad (2.26)$$

where m is the mass of the parcel of gas. In Fig.(2.4), a schematic pV -diagram of the cycle is shown. The work used in the cycle is equal to the area ABCD, and given by

$$\delta W = \int_{ABCD} p dV. \quad (2.27)$$

The used acoustic power in each step is shown in Fig.(2.4). Using the acoustic approximation, $p_1 \ll p_m$, and the Poisson's law for the two adiabatic steps, the result after calculation is

$$\delta W \approx -2p_1 \delta V. \quad (2.28)$$

The volume δV is related to δT by Eq.(2.23),

$$\delta V = (\beta V)_m \delta T. \quad (2.29)$$

Insertion into Eq.(2.28) yields

$$\delta W = -2p_1 (\beta V)_m \delta T. \quad (2.30)$$

In step 3, the parcel of gas moves back to its initial position, expands and cools. At this time, the parcel of gas is colder than the local stack surface, and heat δQ flows into the parcel (step 4).

In case δT is negative, heat flows into the parcel which expands and does work δW on its surroundings (prime mover). The sign of the temperature difference δT (and hence magnitude of ∇T_m) determines, after displacement and compression, the direction of the heat flow, into or out of the parcel of gas. Therefore, the refrigerator mode and prime mover mode can be distinguished by the sign of δT . If the temperature change $2x_1 \nabla T_m$ in the plate just matches the adiabatic temperature change $2T_1$, then the temperature gradient in the stack is named the critical temperature and is given by

$$(\nabla T)_{\text{crit}} = \frac{T_1}{x_1}. \quad (2.31)$$

Using Eq.(2.22) and $x_1 = u_1/\omega$, where u_1 is the gas particles velocity amplitude and ω the angular frequency, we obtain

$$(\nabla T)_{\text{crit}} = \frac{p_1 \omega}{\rho_m c_p u_1}. \quad (2.32)$$

The two modes of operation are characterized in terms of the ratio of the temperature gradient along the stack and the critical temperature gradient

$$\Gamma = \frac{\nabla T_m}{(\nabla T)_{\text{crit}}}. \quad (2.33)$$

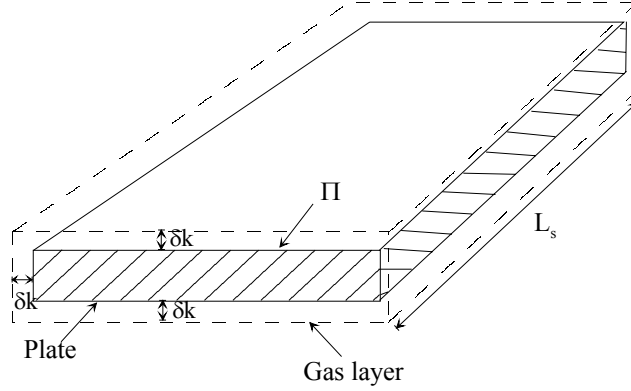


Figure 2.5: A single stack plate of length L_s and perimeter Π . The gas layer at a distance δ_k from the plate is shown by dashed line. The gas area is equal to $\Pi\delta_k$ and the total volume of gas in contact with the plate is $\Pi\delta_k L_s$.

Employing Eqs.(2.33), (2.22) and assuming an ideal gas ($\beta T = 1$) we can rewrite Eqs.(2.26) and (2.30), as

$$\delta Q \approx -2Vp_1(\Gamma - 1), \quad (2.34)$$

and

$$\delta W \approx 4 \left(\frac{p_1^2 V \beta}{\rho_m c_p} \right)_m (\Gamma - 1), \quad (2.35)$$

respectively. As can be seen from Fig.(2.5), if we suppose that Π is the perimeter of the plate in the direction normal to the axis of the resonator, L_s is the length of the plate parallel to the resonator axis (wave direction), and since only the layer of gas at a distance δ_k from the plate contributes to the thermoacoustic heat transport, the effective volume rate of flow of the gas is $\Pi\delta_k u_1$. Here u_1 is the amplitude of the speed of motion of the gas, caused by the sound wave.

The thermoacoustic heat flow rate along the plate from T_C to T_H (refrigerator mode) is obtained by replacing V in Eq.(2.34) by the effective volume flow $\Pi\delta_k u_1$, i.e.

$$\dot{Q} \approx -2\Pi\delta_k p_1 u_1 (\Gamma - 1). \quad (2.36)$$

The total volume of gas that is thermodynamically active along the plate is $\Pi\delta_k L_s$, so that the total work used to transport heat is given by

$$W \approx \frac{4\Pi\delta_k L_s p_1^2 \beta}{\rho_m c_p} (\Gamma - 1). \quad (2.37)$$

The power needed to pump the heat is the work per cycle times the frequency ω , so that

$$\dot{W} \approx \omega \frac{4\Pi\delta_k L_s p_1^2 \beta}{\rho_m c_p} (\Gamma - 1). \quad (2.38)$$

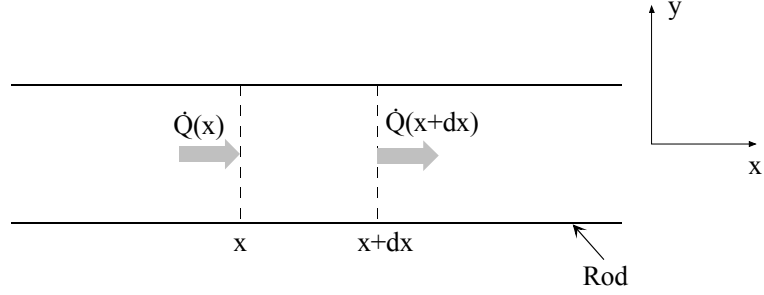


Figure 2.6: *Illustration used in the derivation of the heat conduction equation.*

When use is made of the definition of the speed of sound and the ideal gas law,

$$\begin{aligned} a^2 &= \gamma \frac{p_m}{\rho_m} \\ &= T_m c_p (\gamma - 1), \end{aligned} \quad (2.39)$$

where $\gamma - 1$ is the work parameter of the gas, we can rewrite Eq.(2.38) as

$$\dot{W} \approx \omega \frac{4\Pi\delta_k L_S (\gamma - 1) p_1^2}{\rho_m a^2} (\Gamma - 1). \quad (2.40)$$

A quantitative evaluation of \dot{Q} , and \dot{W} for sinusoidal p_1 and u_1 would give the same results except that each expression has a numerical prefactor of $\frac{1}{4}$ [3]. The total heat flow and absorbed acoustic power in the stack can be obtained by using the total perimeter of the plates Π_{tot} instead of the perimeter of one plate Π .

Expressions (2.36) and (2.38) change sign as Γ passes through unity. Three cases can be distinguished: $\Gamma = 1$, there is no heat flow and no power is needed; When $\Gamma < 1$, the heat is transported against the temperature gradient so that external power is needed, and the device operates as a refrigerator; $\Gamma > 1$, due to the large temperature gradient, work is produced, and the device operates as a prime mover. Therefore, the device can operate as a refrigerator as long as the temperature gradient over the plate (stack) is smaller than the critical temperature gradient (Eq.(2.31)). But we can impose a large temperature gradient over the plate so that the device operates as a prime mover ($\Gamma > 1$).

As stated previously, the thermoacoustic effect occurs within the thermal penetration depth δ_k , which is roughly the distance over which heat can diffuse through the gas in a time $1/\pi f$, where f denotes the frequency of the acoustic wave. In Fig.(2.6), the heat conduction in one dimension through a rod of cross-section A is illustrated. Considering the energy balance for a small element dx of the rod, we suppose that heat is the only form of energy that enters or leaves the element dx , at x and $x + dx$,

and that no energy is generated inside the element. Energy conservation yields

$$\rho_s A \frac{\partial u}{\partial t} = -\frac{\partial \dot{Q}}{\partial x}. \quad (2.41)$$

The heat flow is given by the Fourier's law of heat conduction

$$\dot{Q} = -K_s A \frac{dT}{dx}, \quad (2.42)$$

where K_s is the thermal conductivity of the material. Substituting Eq.(2.42) and the thermodynamic expression $du = c_s dT$ for the internal energy of solid-state material into Eq.(2.41) yields

$$\frac{\rho_s c_s}{K_s} \frac{\partial T}{\partial t} = \frac{\partial^2 T}{\partial x^2} \quad (2.43)$$

where c_s and ρ_s are the isobaric specific heat and density of the material, respectively. If we substitute the characteristic dimensions $\delta_s = x/x'$ and $t' = \omega t$ into Eq.(2.43) we get

$$\frac{\rho_s c_s \omega}{K_s} \frac{\partial T}{\partial t'} = \frac{1}{\delta_s^2} \frac{\partial^2 T}{\partial x'^2}, \quad (2.44)$$

so that

$$\delta_s^2 = \frac{K_s}{\rho_s c_s \omega} \quad (2.45)$$

and hence

$$\delta_s = \sqrt{\frac{\kappa_s}{\omega}}, \quad (2.46)$$

where κ_s is the thermal diffusivity, $\kappa_s = K_s/\rho_s c_s$. A similar procedure can be used to derive an analogous expression for the thermal penetration in a gas. Closely related to the thermal penetration depth is the viscous penetration depth in a gas δ_ν . It is roughly the distance over which momentum can diffuse in a time $\frac{1}{\pi f}$ and it is given by

$$\delta_\nu = \sqrt{\frac{2\nu}{\omega}} \quad (2.47)$$

where the kinematic viscosity ν is given by

$$\nu = \frac{\eta}{\rho}, \quad (2.48)$$

here η is the dynamic viscosity of the gas. An important parameter for the performance of thermoacoustic devices is the Prandtl number σ , which is a dimensionless parameter describing the ratio of viscous to thermal effects

$$\sigma = \frac{\eta c_p}{K} = \left(\frac{\delta_\nu}{\delta_k} \right)^2. \quad (2.49)$$

For most gases (air, inert gases) but not gas mixtures, σ is nearly $\frac{2}{3}$, so that for these gases thermal and viscous penetration depths are quite comparable. The effect of viscosity on the heat flow and acoustic power will be discussed in the next chapter.

2.3 Acoustic concepts

In this section, some acoustic concepts which are important for proper operation of thermoacoustic devices will be described. The discussion will be limited to standing wave thermoacoustic devices, which are more related to the subject of this thesis.

A simple illustration of a thermoacoustic refrigerator is shown in Fig.(2.2). It consists of an acoustic resonator (tube) of length L (along x) and radius r . The resonator is filled with a gas and closed at one end. An acoustic driver, attached to the other end, sustains an acoustic standing wave in the gas, at the fundamental resonance frequency of the resonator. A stack of parallel plates and two heat exchangers are appropriately installed in the resonator.

The first condition for the proper operation of thermoacoustic refrigerators is that the driver sustains an acoustic wave. This means that the driver compensates for the energy absorbed in the system. Hence, a small travelling wave component is superimposed on a standing wave; we have to note that in a pure standing wave there is no energy transport.

To illustrate the acoustics, we consider for simplicity that the stack and the heat exchangers have no effect on the acoustic field in the tube. The driver excites a wave along the x direction. The combination of a plane traveling wave to the right and the reflected wave at the closed end of the tube generates a sinusoidal standing wave. The acoustic pressure in the tube is given by [4, 5]

$$\begin{aligned} p(x, t) &= p_1(x) \sin \omega t, \\ p_1(x) &= p_0 \cos kx \end{aligned} \tag{2.50}$$

where p_0 is the pressure amplitude at the pressure antinodes of the standing wave, ω is the angular frequency of the wave, k is the wave number.

By integration of Newton's second law (acoustic approximation), $\rho \frac{\partial u}{\partial t} = -\frac{\partial p}{\partial x}$, the gas particle velocity is [4, 5]

$$\begin{aligned} u(x, t) &= u_1(x) \cos \omega t, \\ u_1(x) &= \frac{p_0}{\rho_m a} \sin kx \end{aligned} \tag{2.51}$$

where

$$k = \frac{\omega}{a}. \tag{2.52}$$

From the fact that $\sin kx$ is zero where $\cos kx$ is maximum and vice versa, it follows that pressure antinodes are always velocity nodes and vice versa; the pressure and velocity are spatially 90 degrees out-of-phase.

The frequency of the acoustic standing wave is determined by the type of gas, the length L of the resonator and the boundary conditions. A quarter-wavelength resonator is suitable, for many reasons as will be illustrated in chapter 6. But a half-wavelength resonator can also be used. This depends on how the standing wave fits in the tube. A half-wavelength resonator has two closed ends, so that the velocity is zero at the ends and the pressure is maximal (antinodes). The resonance modes are given by the condition that the longitudinal velocity vanishes at the ends of the resonator

$$\sin kL = 0. \quad (2.53)$$

Hence,

$$\lambda = \frac{2L}{n} \quad (n = 1, 2, 3, \dots), \quad (2.54)$$

where

$$k = \frac{2\pi}{\lambda} \quad (2.55)$$

is used. In this case we see that the first (fundamental) mode which is usually used in thermoacoustic devices, corresponds to $L = \lambda/2$, ergo the name half-wavelength resonator.

For a quarter-wavelength resonator, one end is open and the other end is closed. This requires a pressure node at the open end, hence

$$\cos kL = 0, \quad (2.56)$$

so that

$$\lambda = \frac{4L}{2n-1} \quad (n = 1, 2, 3, \dots). \quad (2.57)$$

The fundamental mode corresponds to $L = \lambda/4$, ergo the name quarter-wave resonator. The refrigerator shown in Fig.(2.2), is assumed to be a half-wavelength device. Thus, in the resonance tube, we obtain the pressure and velocity distributions indicated in Fig.(2.2b).

2.4 Basic operation concepts

In the previous sections some basic thermodynamic and acoustic concepts have been introduced. In this section, we will illustrate the effect of the position of the stack in the standing-wave field on the behavior of the thermoacoustic devices.

In Fig.(2.2), some important length scales are also shown: the longitudinal lengths, wavelength $\lambda = 2L$, gas excursion x_1 , stack length L_s , and the mean stack position from the pressure antinode x_s , and the transversal length: spacing in the stack $2\delta_k$. For audio frequencies, we have typically for thermoacoustic devices:

$$\frac{1}{k} = \frac{\lambda}{2\pi} \gg x_s \geq L_s > x_1. \quad (2.58)$$

Since the sinusoidal displacement x_1 of gas parcels is smaller than the length of the plate L_s , there are many adjacent gas parcels, each confined in its cyclic motion to a short region of length $2x_1$, and each reaching the extreme position as that occupied by an adjacent parcel half an acoustic cycle earlier (Fig.(2.3b)). During the first half of the acoustic cycle, the individual parcels move a distance x_1 toward the pressure antinode and deposit an amount of heat δQ at that position on the plate. During the second half of the cycle, each parcel moves back to its initial position, and picks up the same amount of heat, that was deposited a half cycle earlier by an adjacent parcel of gas. The net result, is that an amount of heat is passed along the plate from one parcel of gas to the next in the direction of the pressure antinode as shown in Fig.(2.3b).

Finally, we note that, although the adiabatic temperature T_1 of a given parcel may be small, the temperature difference ΔT_m over the stack can be large, as the "number of parcels", L_s/x_1 , can be large (Fig.(2.3b)). As from Eq.(2.33)

$$\Gamma = \frac{\nabla T_m}{(\nabla T)_{\text{crit}}} = \frac{\frac{\Delta T_m}{L_s}}{\frac{T_1}{x_1}}, \quad (2.59)$$

we find

$$\Delta T_m = \frac{L_s}{x_1} \frac{T_1}{\Gamma}. \quad (2.60)$$

Since $\Gamma < 1$, and $L_s \gg x_1$, we see that ΔT_m can be made much larger than T_1 .

2.4.1 Temperature gradient

The gas harmonic excursion, x_1 is given by

$$x_1 = \frac{u_1}{\omega}. \quad (2.61)$$

Hence, close to a pressure antinode (velocity node) the excursion of a typical parcel of gas is small. At the same time the parcel experiences large changes in pressure and a large adiabatic temperature change T_1 (Eq.(2.22)). So, the critical temperature gradient at that position $(\nabla T)_{\text{crit}} = T_1/x_1$ is large. If we replace u_1 by its expression from Eq.(2.51), we get

$$x_1 = \frac{p_0}{\rho \omega a} \sin kx_s. \quad (2.62)$$

Using Eq.(2.58) yields

$$x_1 = \frac{p_0}{\rho_m a^2} x_s. \quad (2.63)$$

Substituting this result into Eq.(2.31) we obtain

$$(\nabla T)_{\text{crit}} = \gamma \frac{p_m}{p_0} \frac{T_1}{x_s} = (\gamma - 1) \frac{T_m}{x_s}, \quad (2.64)$$

where Eqs.(2.39) en (2.24) have been used. In the refrigerator (heat pump), $(\nabla T)_{\text{crit}}$ is the maximum temperature gradient that can be developed over the stack, which means that close to a pressure antinode, we can expect the largest temperature difference over the stack. Further away from the pressure antinode, pressure and temperature changes become smaller whereas displacements become larger, so the maximum temperature difference that can be reached is smaller.

2.4.2 Heat flow

Eq.(2.36) shows that the heat flow is proportional to the product $p_1 u_1$, and so vanishes if the stack is placed at either a pressure node or a velocity node of the standing acoustic wave. The maximum value of $p_1 u_1$ is at $x = \lambda/8 = L/2$. The factor $(\Gamma - 1)$ appears also in the expression of heat flow. This factor is negative for refrigerators, and its effect can be derived from the discussion in preceding subsection. The lateral section of gas effective for the process $\Pi \delta_k$, can be maximized by using more plates, optimally spaced, in the stack so that the total perimeter Π is as large as possible while maintaining a stack spacing greater than about $2\delta_k$.

2.4.3 Acoustic power

In the absence of viscosity, the expression for the power needed to pump heat, Eq.(2.40), is similar to that of heat flow, the only difference is the presence of the work parameter $(\gamma - 1)$. Since each parcel along the plate absorbs net work, the total work done on the gas is proportional to the plate length L_s .

2.4.4 Viscosity

The discussion above concerns an inviscid gas. When viscosity is taken into account, the resulting expressions are much more complicated. These expressions will be presented in the following chapter. As indicated in the end of section 2.2, the viscous penetration depth is nearly as large as the thermal penetration depth, so most of the gas in the stack experiences significant viscous shear. However, the definition of the critical temperature gradient (Eq.(2.32)) will be kept throughout this thesis. In fact, with viscosity present, there is a lower critical temperature gradient below which the engine pumps heat and a higher critical gradient above which the engine is a prime mover. Between these two limiting gradients the engine is in a useless state, using work to pump heat from hot to cold.

2.4.5 Performance

At this stage, an estimation of the theoretical performance of the thermoacoustic devices, using an inviscid working gas, can be calculated from the expression of COP (η) derived in section 2.1 in combination with the heat and work equations of section 2.2. The COP is given by

$$COP = \frac{\dot{Q}}{\dot{W}}. \quad (2.65)$$

Making use of Eqs.(2.32), (2.36), (2.38) and $\Delta T_m = \nabla T_m L_s$ yields

$$COP = \Gamma \frac{T_m}{\Delta T_m} = \Gamma COP_C. \quad (2.66)$$

Here COP_C is Carnot's coefficient of performance (Eq.(2.11)), the maximum possible performance of a refrigerator at T_m spanning the temperature difference ΔT_m . We see that COP_C is approached as $\Gamma \rightarrow 1$, in which case heat and work are zero.

We note that standing-wave thermoacoustic devices are intrinsically irreversible. The irreversible heat transfer δQ across the temperature difference δT , steps 2 and 4 in Fig.(2.3), is essential to the operation of these devices. They do rely on the imperfect thermal contact across the thermal penetration depth δ_k , which provides the necessary phasing between displacement and thermal oscillations. This is the reason why the performance of standing wave thermoacoustic devices falls below Carnot's performance. The performance will be degraded furthermore if viscous, thermal conduction, and other losses in the different parts of the device will be considered. To date, the best performance reached with such devices is about 20 % of Carnot [6].

2.5 Some basic measurements

In this section some basic thermoacoustic measurements, using an experimental set-up similar to that illustrated in Fig.(2.2), will be introduced. These results will be used to demonstrate the effects discussed in the foregoing sections.

2.5.1 Set-up

A demonstration refrigerator has been built which consists of a Polyvinyl chloride (PVC) tube of length 70 cm, and inner diameter 4.2 cm, as illustrated in Fig.(2.7). The whole system is made of PVC which makes it light, easy to build and transport. The resonator is filled with air at atmospheric pressure. The stack consists of parallel drinking straws, of inner diameter 2 mm. The stack has a diameter of 4.2 cm and a length of 7.9 cm, and can easily be installed inside the resonator tube. At one end the resonator is driven by a commercially available loudspeaker. This driver is

mounted in a PVC-housing to which the resonator is connected. The other end of the resonator is closed by a thick removable cover plate. The system is not thermally insulated, and can simply be set on a table to demonstrate thermoacoustic cooling. So, the measurements are qualitative.

The acoustic pressures are measured using microphones. One is permanently installed near the driver end, and one can also be placed on the closed end. To measure the pressure distribution along the resonant tube, a microphone is mounted on the end of a hollow 2 mm diameter stainless steel tube. The tube serves both to allow a free positioning of the microphone inside the resonance tube and to extract the microphone leads; it passes through a cork that is fixed in a hole on the closed end of the resonator in order to keep acoustic losses low. The pressure transducer, placed near the driver end, measures the dynamic pressure and is used for determining the resonance frequency.

A copper-constantan thermocouple is used to measure the temperature difference over the stack. As illustrated in Fig.(2.7c), the temperature difference is measured by fixing each copper-constantan junction of the thermocouple on opposite ends of the stack. Also, two-terminal IC temperature transducers, type AD590 JH, are used to measure separately the temperatures of the hot and cold ends of the stack during operation.

In order to measure the temperature difference over the stack as function of position inside the resonance tube, the same procedure is used for the measurement of the pressure distribution. The stack can be mounted on the end of a hollow 3 mm diameter stainless steel tube which allows the positioning of the stack at different places inside the resonance tube, as shown in Fig.(2.7c).

The signals from the thermocouple and the IC-thermometers are measured by a multimeter, and the dynamic pressure by a lock-in amplifier. The driver is powered by a function generator in combination with a power amplifier. The data acquisition is controlled by a computer, which controls and interrogates the different instruments via a GPIB interface.

2.5.2 Measurements

First, the acoustic resonance frequency is determined, by making a low-power frequency sweep. The dynamic pressure signal is recorded over the sweep interval. From this resonance spectrum, the resonance frequency is determined. Then, at this resonance frequency, the pressure distribution in the resonance tube is measured by positioning the microphone, as discussed above, inside the tube. Finally, the temperature difference, developed across the stack, is recorded as function of the position of the

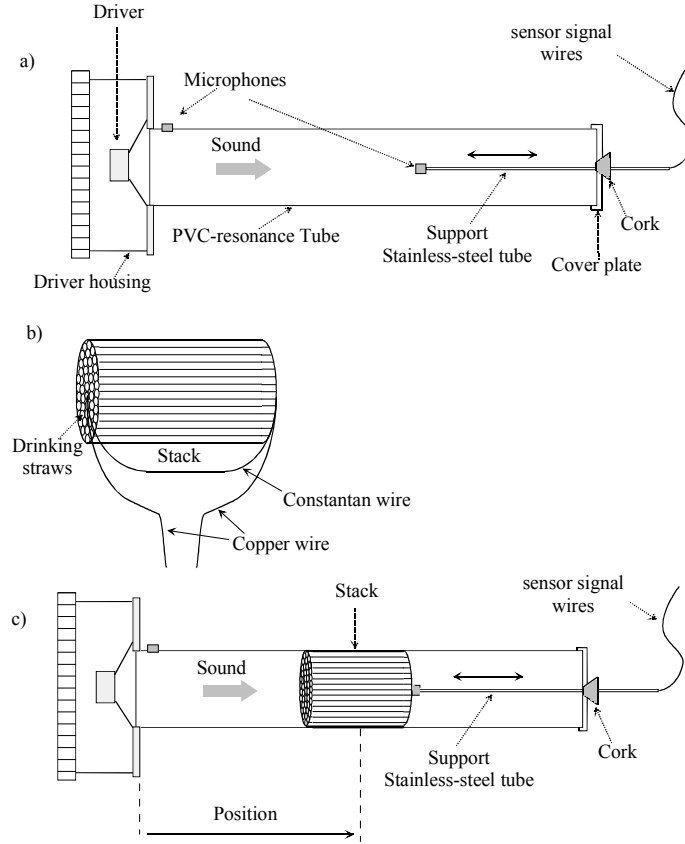


Figure 2.7: a) Set-up used to measure the acoustic pressure distribution. b) The stack is made of drinking straws glued together. A constantan-copper thermocouple is used to measure the temperature difference over the stack. c) Set up used to measure the temperature difference over the stack as function of position.

stack. The measurements were all made with air at atmospheric pressure, near room temperature (23 °C), and at resonance.

A typical measurement result is presented in Fig.(2.8). The standing wave acoustic pressure distribution inside the resonance tube is shown in Fig.(2.8a). The acoustic pressure node and antinodes, corresponding with the resonance frequency, are also indicated in the graph, along with the expected heat flow directions as discussed in Section 2.2. It was concluded that in the heat pump regime, heat flows always towards the nearest pressure antinode.

The measurements of the heating and cooling at the ends of the stack as a function of time, at a position of 21.5 cm from the driver end, are displayed in Fig.(2.8b). In this graph, T_{Hot} is the temperature of the hot side of the stack, which faces the pressure antinode side. T_{Cold} is the temperature of the cold side of the stack, which

faces the pressure node side. Initially, the temperature of the two ends of the stack was the same (23 °C). After turning on the loudspeaker (time zero) T_{Hot} increases, and T_{Cold} decreases until a steady state is reached in about seven minutes. What actually happens at the ends of the stack when the driver is turned on is that heat flows out of one end of the stack, and into the other end of the stack, as discussed in section 2.2. Thus, the end that supplies heat cools down and the other end, which absorbs heat, warms up. The thermoacoustic heat transport is maximum at the start of the measurement when there is no temperature gradient over the stack. As the temperature gradient develops, the heat flow diminishes. A steady state temperature is reached when the thermoacoustic heat flow in the gas is balanced by a return diffusive heat flow in the stack and in the gas. Since the acoustic power used to transport heat shows up as dissipative heat at the hot side of the stack, one can expect a higher temperature increase at the hot side than the temperature decrease at the cold side, according to Eq.(2.6). The temperature difference across the stack, $T_{\text{Hot}} - T_{\text{Cold}}$, corresponding to graph (2.8b), is shown in Fig.(2.8d) as a function of time.

An example of the temperature difference over the stack as function of the distance from the loudspeaker end in air at atmospheric pressure, at the resonance frequency of the tube, at an ambient temperature of 23 °C, and with a driving ratio, D , of 2.2 % is shown in Fig.(2.8c). The drive ratio is defined as the ratio of the acoustic peak pressure amplitude to the mean pressure of the gas.

Graph (2.8c), shows that the temperature difference changes sign as the pressure gradient changes sign. As discussed above, the heat flow is always in the direction of the pressure antinode in the refrigeration mode. There is essentially a sinusoidal dependence of the temperature difference on position with zeros at both pressure and velocity nodes (or antinodes), since heat flow vanishes. This follows from the product $p_1 u_1$ in Eq.(2.36). The temperature difference indicates a sawtooth shape instead of a sinusoid, with the maxima shifted toward the pressure antinodes. This is a consequence of the high drive ratio of 2.2 %. A more accurate study of the temperature difference over a small stack named the thermoacoustic couple for low driving ratios of 0.3 % has been done by Wheatly et al. [7]; in that case the temperature difference was a perfect sinusoid. Measurements have also been done by Atchley et al.[8] for drive ratios from approximately 0.1 % to 2 %, in argon and helium having different mean pressures, and it is found that the temperature difference progresses from a sinusoid to a sawtooth curve and the maximums shift towards the pressure antinodes at approximately a drive ratio of about 1.03 %. Our measurements were made at a drive ratio of 2.2 %, so a sawtooth shape for the temperature difference can be expected.

In summary, we conclude from the measurements that in a thermoacoustic refrigerator (heat pump), heat flows always toward the closest pressure antinode, making

that end of the stack hottest. However, at both the pressure antinodes and nodes there is no flow of heat ($\Delta T = 0$). Hence, the position of the stack in the resonator tube relative to the standing wave is an important factor in the design of the standing wave thermoacoustic devices. A detailed discussion of these effects will be given in chapter 6.

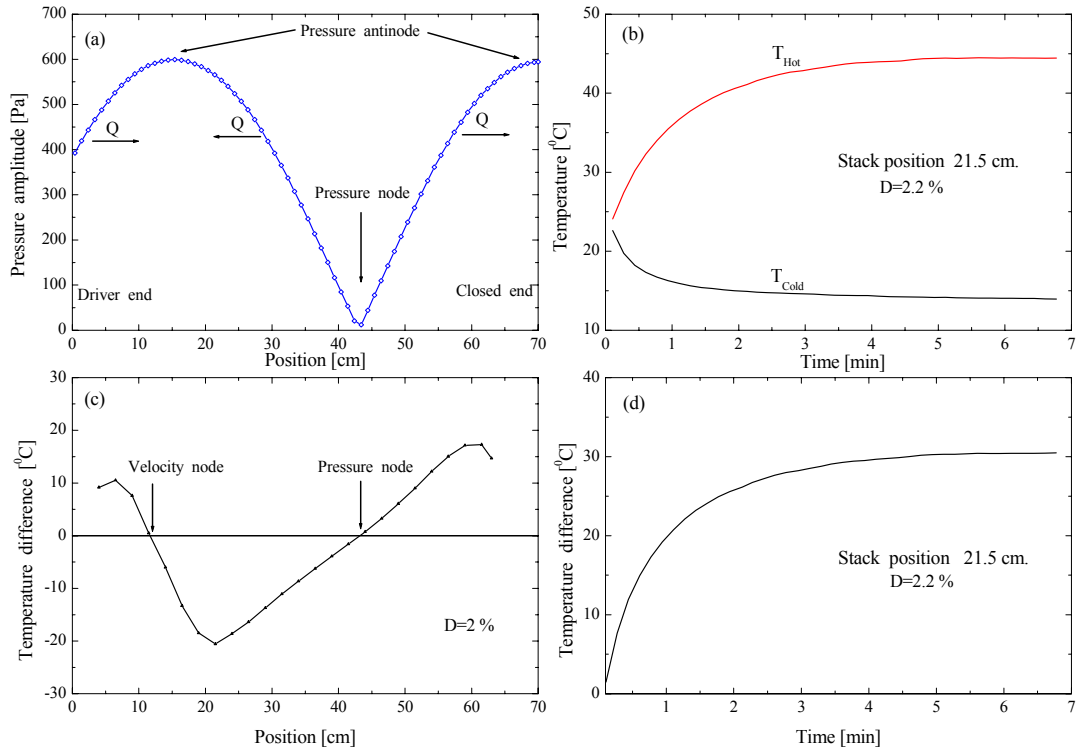


Figure 2.8: A typical experimental result. (a) The pressure distribution inside the resonator at the resonance frequency, the pressure node and antinode along with the heat flow direction are indicated in the graph. (b) The temperature of the hot and cold sides of the stack as functions of time at a fixed position of 21.5 cm from the loudspeaker. (c) The temperature difference ($T_{Hot} - T_{Cold}$) across the stack as function of position from the loudspeaker end. (d) The temperature difference across the stack as a function of time corresponding to the same stack location as (b).